

Understanding Proton Emission in Central Heavy-Ion Collisions

D. O. Handzy, W. Bauer, F. C. Daffin, S. J. Gaff, C. K. Gelbke, T. Glasmacher, E. Gualtieri, S. Hannuschke, M. J. Huang, G. J. Kunde, R. Lacey,* T. Li, M. A. Lisa,[†] W. J. Llope,[‡] W. G. Lynch, L. Martin, C. P. Montoya,[§] R. Pak, G. F. Peaslee,^{||} S. Pratt, C. Schwarz,[¶] N. Stone, M. B. Tsang, A. M. Vander Molen, G. D. Westfall, J. Yee, and S. J. Yennello**

*National Superconducting Cyclotron Laboratory and Department of Physics and Astronomy,
Michigan State University, East Lansing, Michigan 48824*

(Received 4 April 1995)

Two-proton correlation functions for central collisions of $^{36}\text{Ar} + ^{45}\text{Sc}$ at $E/A = 80, 120,$ and 160 MeV are compared to calculations with the Boltzmann-Uehling-Uhlenbeck (BUU) transport model. Agreement is found at $E/A = 80$ MeV, but the model predicts too large correlations at $E/A = 120$ and 160 MeV. The discrepancy may be due to delayed emission of protons from particle-unstable states not modeled in BUU.

PACS numbers: 25.70.Pq

Two-proton correlation functions provide a means for viewing the space-time development of heavy-ion collisions [1–3]. For energies below a few tens of MeV per nucleon, where long-lived evaporative emission is expected, measured two-proton correlation functions were found to be consistent with compound-nucleus model predictions [4,5]. At high energies, above 200 MeV per nucleon, nuclei should be vaporized and semiclassical cascades should provide a valid description. For collisions at intermediate energies, nuclei disintegrate by emitting a large number of light clusters and intermediate mass fragments. As this energy range represents the transition from liquidlike to gaslike behavior it may be the most interesting region to study, but it is also the most difficult region to model theoretically.

Semiclassical simulations based on the Boltzmann-Uehling-Uhlenbeck (BUU) model are thought to provide a reasonable picture of the global dynamics of a collision [6]. The model generates Pauli-blocking effects and mean fields by sampling many test particles, which effectively washes out fluctuations. BUU calculations were successful in reproducing two-proton correlation functions measured at energies below about 100 MeV per nucleon [4,7–10]. For central $^{36}\text{Ar} + ^{45}\text{Sc}$ collisions at 80 MeV per nucleon, detailed dependences of the measured two-proton correlation function on the total momentum of the proton pair and on the orientation of the relative momentum were remarkably well reproduced by BUU calculations [8]. Emerging discrepancies for peripheral collisions were attributed to an inadequate treatment of the nuclear surface [8], but not to a fundamental limitation of the BUU approach. Rather surprisingly, the model failed to explain inclusive measurements for $^{40}\text{Ar} + ^{197}\text{Au}$ collisions at 200 MeV per nucleon [10] where it should have been on firm theoretical ground. The experimental correlation function at 200 MeV displayed little sensitivity to the protons' energy, while BUU calculations predicted the opposite [10]. Improved agreement was obtained by using two-proton emission probabilities calculated

with the quantum molecular dynamics (QMD) model [10,11], but such calculations could not reproduce [10] the correlation functions measured [9] at 60 MeV per nucleon and, hence, did not resolve the problem. In addition, the correlation function at 200 MeV displayed a filling of the minimum at relative momentum $q \approx 0$, not observed at lower energies and not reproduced by theory.

In this Letter we report experimental results for central collisions, key to studies of hot nuclear matter, at $E/A = 80, 120,$ and 160 MeV. We chose a more symmetric system, $^{36}\text{Ar} + ^{45}\text{Sc}$, to allow for improved impact-parameter selection [12]. BUU calculations predict shorter emission time scales and hence smaller apparent source sizes as the beam energy is increased. These predictions are not confirmed experimentally, and clear discrepancies between theory and experiment are observed at the two higher energies. We argue that the failure of the model may be attributable to delayed emission from particle unbound states—a quantum effect not included in the BUU theory.

The experiments were performed at the National Superconducting Cyclotron Laboratory at Michigan State University (MSU). From the K1200 cyclotron, beams of ^{36}Ar ions of 80, 120, and 160 MeV per nucleon energy were focused on ^{45}Sc targets of area density 10, 40, and 40 mg/cm², respectively. Charged particles were detected in 209 plastic ΔE - E phoswich detectors of the MSU 4π array [13], which covered angles between 5° and 164° in the laboratory frame. Particles stopped in the slow E scintillators were identified by particle type and energy, with calibration uncertainty of about 10%. One hexagonal module of the 4π array, centered at $\theta_{\text{lab}} = 38^\circ$, was replaced by a hodoscope [5,14] of 56 ΔE - E telescopes covering the angular range of $\theta_{\text{lab}} = 30^\circ$ – 45° [8]. Each telescope consisted of a 300 or 400 μm silicon ΔE - E detector backed by a 10 cm CsI(Tl) E detector and subtended a solid angle of $\Delta\Omega \approx 0.37$ msr. The nearest-neighbor spacing between telescopes was $\Delta\theta = 2.6^\circ$. The energy resolution for each telescope was about 1% for 50 MeV

protons. Both two-proton coincidence and singles events in the hodoscope were recorded in coincidence with data from the 4π array. An impact-parameter scale was established from the total transverse kinetic energy [8,15] measured in the 4π array, and central collisions were selected by the cut $b/b_{\max} \leq 0.3$.

The solid points in Fig. 1 show the singles energy spectra of protons detected at $\langle \theta_{\text{lab}} \rangle = 31^\circ$; histograms show BUU predictions. The BUU calculations overpredict the low-energy proton yield, but they reproduce the approximate shape of the high-energy tail. The overprediction of proton yields at low energy has been observed before and attributed to the model's inability to treat the formation of bound clusters [16]. Clusters should form preferentially in regions of phase space where the nucleon population density is high, hence more protons should be "lost" to bound clusters at lower than at higher proton energy.

Figure 2 shows experimental (points) and theoretical (curves) correlation functions gated on total center-of-mass momentum, $P_{\text{c.m.}} = |\mathbf{p}_1 + \mathbf{p}_2|$, of the detected proton pairs. The experimental correlation function, $1 + R(q)$, was defined in terms of the two-proton coincidence yield, $Y_2(\mathbf{p}_1, \mathbf{p}_2)$, and the proton singles yield, $Y_1(\mathbf{p})$:

$$\sum Y_2(\mathbf{p}_1, \mathbf{p}_2) = C[1 + R(q)] \sum Y_1(\mathbf{p}_1)Y_1(\mathbf{p}_2). \quad (1)$$

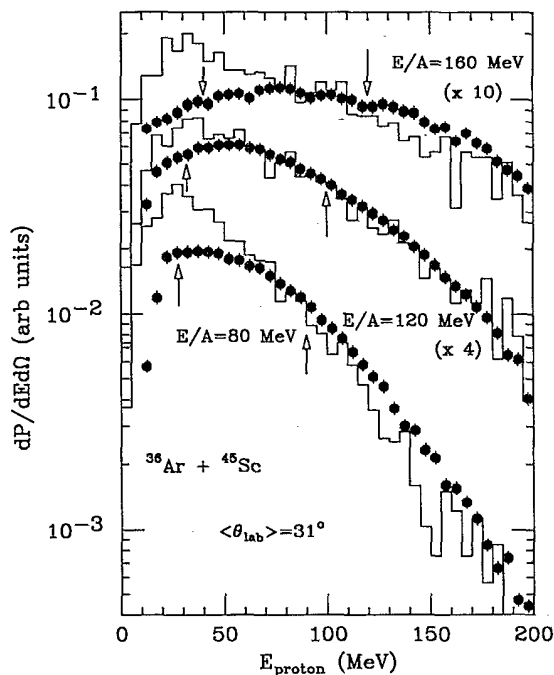


FIG. 1. Laboratory frame proton energy spectra measured at $\theta_{\text{lab}} = 31^\circ$ for central ($b/b_{\max} \leq 0.3$) collisions of $^{36}\text{Ar} + ^{45}\text{Sc}$ at $E/A = 80, 120,$ and 160 MeV (solid points) are compared with the predictions of BUU (histograms). Relative normalization gives equal areas for measured and predicted spectra for $E_{\text{proton}} \geq 50$ MeV. The arrows indicate average values of $E_{\text{proton}}^{\text{lab}}$ corresponding to low and high momentum cuts used to analyze the correlation function in Fig. 2.

Here, p_i is the momentum of proton i , and q is the (invariant) magnitude of the relative momentum four-vector, nonrelativistically: $q = \frac{1}{2}|\mathbf{p}_1 - \mathbf{p}_2|$. For a given experimental gating condition, the sums on each side of Eq. (1) extend over all proton energies and detector combinations of the 56-element hodoscope corresponding to each q bin. The normalization constant C is defined such that $\langle R(q) \rangle = 0$ for $60 \leq q \leq 80$ MeV/c.

At all three energies, the measured maximum of $1 + R(q)$ at $q \approx 20$ MeV/c is larger than for the Ar + Au reaction at $E/A = 200$ MeV [10], and the minimum at $q \approx 0$ is clearly observed for both cuts on $P_{\text{c.m.}}$ [17]. The dependence on $P_{\text{c.m.}}$ is pronounced at $E/A = 80$ MeV [8], but weak at $E/A = 160$ MeV [18]. This latter observation is consistent with the trend observed [10] in the inclusive Ar + Au data.

Theoretical two-proton correlation functions were calculated with the Koonin-Pratt formula, which relates the one-body phase space distribution (predicted by BUU) with the correlation function [1,3,4,7]. The BUU calculations (filtered for experimental acceptance and energy thresholds) were performed with a stiff equation of state ($K = 380$ MeV) and in-medium nucleon-nucleon cross sections set equal to their free values, $\sigma_{NN} = \sigma_{NN}^{\text{free}}$. A proton was considered emitted if it was located in a region of local mass density less than the freeze-out density $\rho_f = \rho_0/8$, where ρ_0 is the density of normal nuclear density. These values of K , σ_{NN} , and ρ_f were used

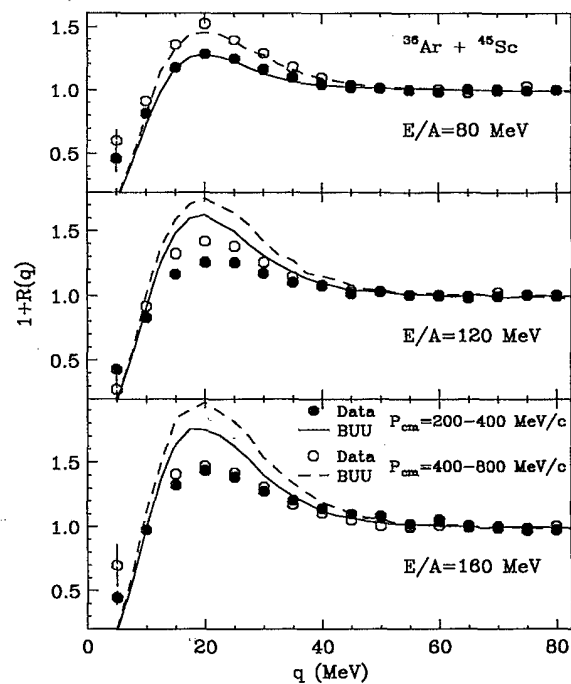


FIG. 2. Two-proton correlation functions for central collisions of $^{36}\text{Ar} + ^{45}\text{Sc}$ at $E/A = 80$ MeV (top), 120 MeV (middle), and 160 MeV (bottom). The momentum cuts employed are indicated in the figure.

[4,7,8] in previous successful descriptions of correlation functions measured at $E/A < 100$ MeV. The BUU calculations reproduce the data at $E/A = 80$ MeV [8], but unexpectedly fail at the two higher energies.

The BUU predictions can be understood from the proton-emission rates, dP/dt , calculated for central $^{36}\text{Ar} + ^{45}\text{Sc}$ collisions; see Fig. 3. At 80 MeV per nucleon, the BUU calculations predict the existence of a long-lived residue [8], which cools by particle emission. In contrast, at the higher energies, a fast flash of nucleon emission is predicted, without residue. While this drastically different scenario leaves no obvious signal in the single-particle spectra shown in Fig. 1, it results in enhanced two-proton correlations—at variance with the data. The near degeneracy of low and high momentum correlation functions at $E/A = 160$ MeV, also not reproduced by the calculations, may indicate that low- and high-energy protons are emitted on similar time scales, and that there is no evaporative cooling of the source.

We explored whether different BUU input parameters would lead to better agreement with the data. Since sensitivities to the stiffness of the equation of state are small [4,7], we performed calculations for different choices of freeze-out density ($\rho_f = \rho_0/8$, $\rho_0/16$, and $\rho_0/32$) and for a density dependent [19] in-medium cross section, $\sigma_{NN} = (1 + \alpha \rho/\rho_0) \sigma_{NN}^{\text{free}}$. The choice of $\alpha = -0.2$ provided the best agreement with the balance energy in collective flow data [19]. We therefore performed calculations for $\alpha = 0, -0.2, -0.4$. Changes in the correlation functions due to these parameter variations were much smaller than the discrepancies between theory and experiment shown in Fig. 2. We thus conclude that the BUU model is inherently deficient in its description of the emitted proton phase space distribution; proton emission is slower (or from a larger source) than predicted.

The lack of fragment formation in the current BUU formalism may be responsible for its substantial overpre-

dition of the correlation functions at $E/A = 120$ and 160 MeV. At the energies under consideration, high-lying particle-unstable states may play an important role in proton production by extending the time scale τ over which protons are emitted. Such delayed emissions are known to exist [9,20], but their magnitude is unknown. We have performed a schematic simulation of such effects by taking a fraction f of the protons predicted to be emitted by BUU and delaying their emission for a time τ , statistically distributed according to $dP/dt = e^{-t/\tau}$. We chose values of τ between 40 to 240 fm/c, corresponding to resonances of widths between approximately 0.8 and 5 MeV. Examples of simulations that reproduce the magnitude of the experimental correlation function at $E/A = 160$ and 120 MeV are shown in the top and bottom panels of Fig. 4. The insets indicate the ranges of τ and f that give similarly good agreement with the data; to some extent, smaller fractions f of delayed particles can be compensated by longer delay times τ .

While the correlation functions are consistent with a delayed proton-emission component, its magnitude is uncertain and not well determined by our schematic simulation [21]. In order to assess whether the range of parameters shown in the insets of Fig. 4 is compatible with statistical expectations, we have performed calculations with the statistical codes firestreak [22] and FREESCO [23] to estimate

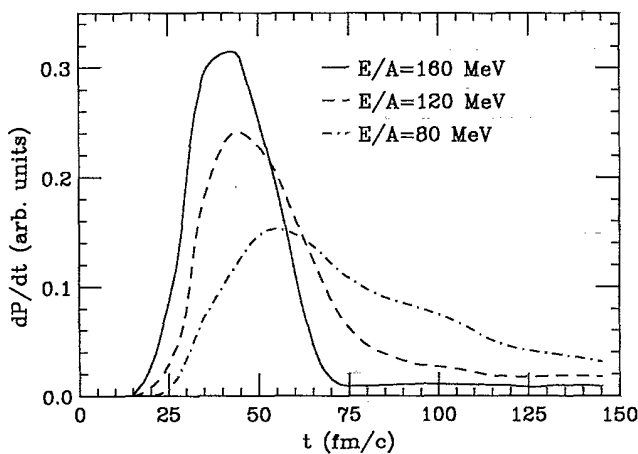


FIG. 3. Proton-emission rates predicted by BUU calculations for central $^{36}\text{Ar} + ^{45}\text{Sc}$ collisions at $E/A = 80, 120,$ and 160 MeV.

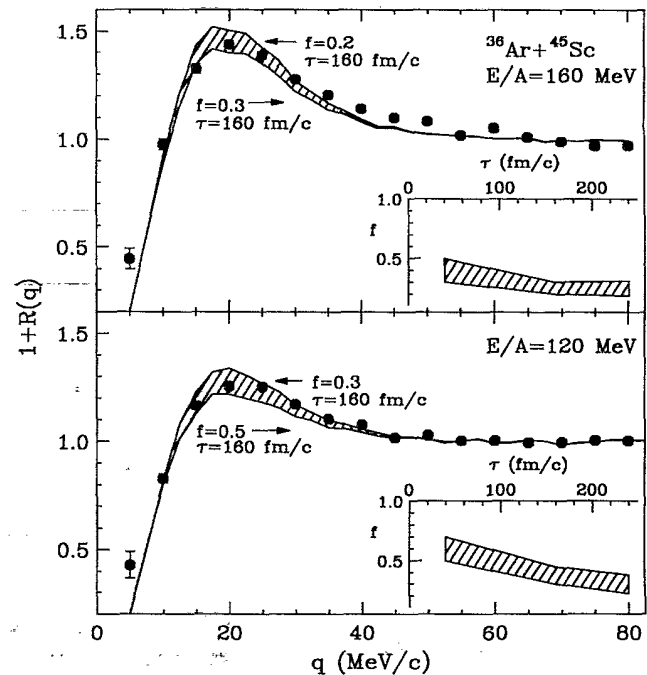


FIG. 4. Two-proton correlation functions (for low-momentum cut) for central collisions of $^{36}\text{Ar} + ^{45}\text{Sc}$ at $E/A = 160$ MeV (top panel) and 120 MeV (bottom panel). Data are shown by points; calculations are described in the text. The insets depict the parameter ambiguity.

sequential-decay contributions to the proton yield. For a single source containing 81 nucleons, using $\rho_f = \rho_0/8$ and $T_f = 8$ MeV, the firestreak model predicts that about 50% of the emitted protons come from resonances; the FREESCO prediction is slightly less than 20% [24]. This range, from the insets of Fig. 4, is qualitatively consistent with values of τ between 50 and 200 fm/c, or widths between 1 and 4 MeV, which are typical of light resonances such as ${}^5\text{Li}^*$ and α^* .

The successful reproduction of the experimental correlation function at $E/A = 80$ MeV by BUU calculations, without an *ad hoc* introduction of resonances, may be due to the predicted formation of a heavy residue, emitting protons over a similar time scale. The observed agreement of QMD calculations with impact-parameter averaged data at $E/A = 200$ MeV and the disagreement at lower energy [10] may be coincidental because QMD does not properly contain the particle-unstable resonances found to be important.

In summary, two-proton correlation functions were measured for central ${}^{36}\text{Ar} + {}^{45}\text{Sc}$ collisions at beam energies of 80, 120, and 160 MeV per nucleon. For the two higher beam energies, the BUU transport theory predicts too large correlations, i.e., proton emission from a more compact space-time geometry than observed experimentally. This deficiency of the theory is likely due to its inability to treat the population of particle unbound resonances and their decay via delayed particle emission. We conclude that proton (and hence nucleon) production in medium-energy heavy-ion collisions is not yet well understood theoretically.

This work was supported by the National Science Foundation under Grants No. PHY-89131815, No. PHY-9403666, and No. PHY-9214992. W.B. acknowledges the support from the NSF Presidential Faculty program, and G.J.K. acknowledges the support of the Alexander-von-Humboldt Foundation.

*Present address: Department of Chemistry, State University of New York, Stony Brook, NY 11776.

[†]Present address: Lawrence Berkeley Laboratory, Berkeley, CA 94720.

[‡]Present address: T.W. Bonner Nuclear Laboratory, Rice University, Houston, TX 77251.

[§]Present address: Merrill Lynch, World Financial Center, North Tower, New York, NY 10281.

^{||}Present address: Department of Chemistry, Hope College, Holland, MI 49423.

[¶]Present address: GSI, Postfach 110552, D-64220 Darmstadt, Germany.

**Present address: Cyclotron Institute, Texas A&M University, College Station, TX 77843.

- [1] S. E. Koonin *et al.*, Phys. Lett. **70B**, 43 (1977).
- [2] D. H. Boal, C. K. Gelbke, and B. K. Jennings, Rev. Mod. Phys. **62**, 553 (1990).
- [3] W. Bauer, C. K. Gelbke, and S. Pratt, Annu. Rev. Nucl. Part. Sci. **42**, 77 (1992).
- [4] W. G. Gong *et al.*, Phys. Rev. C **43**, 1804 (1991).
- [5] A. Elmaani *et al.*, Phys. Rev. C **48**, 2864 (1993).
- [6] G. F. Bertsch and S. Das Gupta, Phys. Rep. **160**, 189 (1988).
- [7] W. G. Gong *et al.*, Phys. Rev. C **43**, 781 (1991).
- [8] M. A. Lisa *et al.*, Phys. Rev. Lett. **70**, 3709 (1993); D. O. Handzy *et al.*, Phys. Rev. C **50**, 858 (1994).
- [9] J. Pochodzalla *et al.*, Phys. Rev. C **35**, 1695 (1987).
- [10] G. J. Kunde *et al.*, Phys. Rev. Lett. **70**, 2545 (1993).
- [11] J. Aichelin, Phys. Rep. **202**, 233 (1991).
- [12] M. B. Tsang *et al.*, Phys. Rev. C **40**, 1685 (1989).
- [13] G. D. Westfall *et al.*, Nucl. Instrum. Methods Phys. Res., Sect. A **238**, 347 (1985).
- [14] W. G. Gong *et al.*, Nucl. Instrum. Methods Phys. Res., Sect. A **268**, 190 (1988); **287**, 639 (1990).
- [15] L. Phair *et al.*, Nucl. Phys. **A548**, 489 (1992); **A564**, 453 (1993).
- [16] W. G. Gong *et al.*, Phys. Rev. C **47**, R429 (1993).
- [17] The approximate momentum gates used in Ref. [10] were $P_{c.m.} \approx 160\text{--}340$, $340\text{--}430$, and $430\text{--}570$ MeV/c; no minimum at $q \approx 0$ was observed for the two higher gates.
- [18] For the low momentum cut, $\langle\theta_{c.m.}\rangle$ and $\langle P_{c.m.}\rangle$ change from about 90° to 115° and from 323 to 345 MeV/c, respectively, as the beam energy is increased from $E/A = 80$ to 160 MeV; for the high momentum cut, $\langle\theta_{c.m.}\rangle$ and $\langle P_{c.m.}\rangle$ change from 55° to 75° and from 514 to 552 MeV/c.
- [19] W. Bauer *et al.*, Phys. Rev. C **48**, 1982 (1993).
- [20] G. J. Kunde *et al.*, Phys. Lett. B **272**, 202 (1991).
- [21] Slightly larger resonance contributions are needed at $E/A = 120$ MeV than at 160 MeV; because of the schematic nature of our calculations, this result should not be overinterpreted.
- [22] G. D. Westfall *et al.*, Phys. Rev. Lett. **37**, 1202 (1976); J. Gosset *et al.*, Phys. Rev. C **18**, 844 (1978).
- [23] G. Fáí and J. Randrup, Nucl. Phys. **A381**, 557 (1982); Nucl. Phys. **A404**, 551 (1983).
- [24] The two predictions differ because FREESCO incorporates more resonances than firestreak; for details see Refs. [22] and [2].